

Theoretical investigation of the effect of the duct cross-sectional area on the heat transfer and fluid flow

Dr. Ahmed. F. Khudheyer

Miss. Suha K. Jebir

1. Abstract:

For a non-Newtonian fluid in the thermal entrance region for a triangular, square, sinusoidal ducts, the numerical solutions for laminar heat transfer with a constant wall temperature the elliptic grid generation technique was used to transform the continuity equation and the parabolic forms of the energy and momentum equations in Cartesian coordinates to a new form of non-orthogonal coordinates with the boundary of the duct coinciding with the coordinates surface, and then these governing equations are solved by the finite difference technique. Heat transfer and fluid flow results are found for multi-shapes of ducts such as (triangular, square, sinusoidal and four cusped cross sectional area). The effects of axial conduction, viscous dissipation and thermal energy sources with the fluid are neglected. The present results had an excellent agreement with the previous results.

Nomenclature

A	Duct cross-sectional area
D_h	Hydraulic diameter; $4A/P$
G_z	Graetz number; $1/Z$
J	Jacobian; $J = x_\xi y_\eta + y_\xi x_\eta$
Nu	Nusselt number; $h.D_h/k$
p	Fluid static pressure
P	Perimeter of cross section
Re	Reynolds number for the duct; $u.D_h/\nu$
T	Temperature; °C
u	Axial fluid velocity in the duct
U	Dimensionless axial fluid velocity in the duct
x, y, z	Rectangular Cartesian coordinates
X, Y	Dimensional transverse coordinates, $X=x/D_h$; $Y=y/D_h$
Z	Dimensional axial coordinate; $z=(Z/(Re.Pr.D_h))$
α, β, γ	Dimensional transformed functions
ζ, η	Dimensional transformed coordinates
μ	Dynamic viscosity
ν	Kinematic viscosity
θ	Dimensionless temperature

Subscripts

b	Bulk mean
T	Fully developed flow
i	Initial
m	Mean

2. Introduction

The most common heat exchangers employed in many industries such as food, polymer, rubber and biological industries, in these industries use the circular and rectangular ducts, which are easy to maintain. The other arbitrary shaped cross-section ducts are not preferred because of the difficulty of manufacturing and cleaning. There is insufficient research on laminar non-Newtonian fluid flow through irregular boundary ducts. Studies of this type of fluid flow in circular, triangular, trapezoidal and pentagonal ducts are available in the literature, sinusoidal ducts and square ducts with four intended corners have not been studied previously.

Laminar flow solutions for Newtonian fluids were studied by [Shah and London 1982] and [Porter 2002] in an exclusive manner. [Shah and London 1982] solved the fully developed problem for Newtonian laminar heat transfer, solved the thermal entry length problem for a rectangular ducts by using the explicit finite difference method. Entrance region heat transfer in rhombic ducts has been studied by [Asako & Faghri 1988] for a Newtonian fluid by algebraic coordinate transformation.

Hydrodynamically developed channel flow and heat transfer to power-law fluids have been studied by [Ashok & Sastri 2001] for square duct under three thermal boundary conditions. Entrance region non-isothermal flow and heat transfer to power-law fluids have been studied by [Lawal & syrjala 1995] studied the case of fully developed laminar flow of the power-law non-Newtonian fluid in a rectangular duct by using the finite element method.

In the present study, the two cases of Newtonian and non-Newtonian fluid flow through the duct geometries mentioned above are studied. A computer algorithm was developed for both cases. Numerical results are present for square, triangular, four-cusped, rhombic, sinusoidal ducts and for special case of a square duct with four intended corners, as shown in Fig.1.

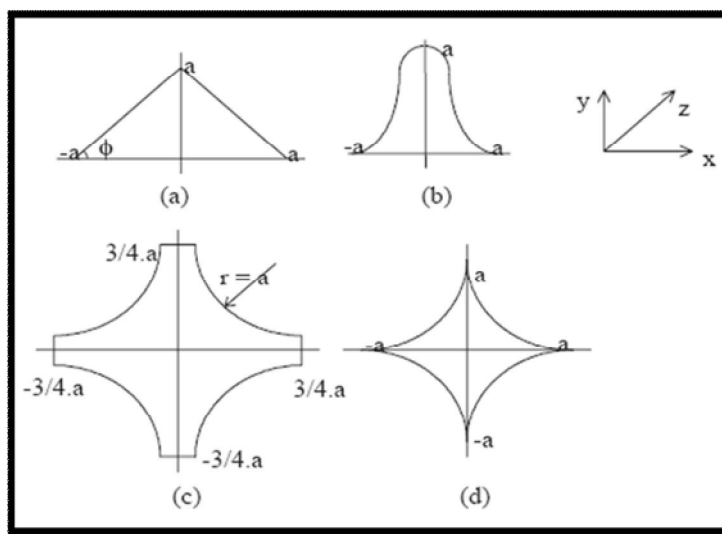


Fig.1 Ducts of arbitrary cross-sections; a)triangular; b)sinusoidal; c)square duct with intended four-corners; d)four-cusped duct.

3. Governing equations:

In this study, the governing equations have the conditions of steady, fully developed, laminar and purely viscous non-Newtonian fluid flow and heat transfer in power-law fluids in horizontal ducts of arbitrary cross-sections. The coordinate system and duct configurations are shown in Fig.2. Both the velocity and temperature distributions are assumed to be uniform at the entrance and hydrodynamically developed and thermally developing laminar flow is analyzed for a non-Newtonian fluid flow through a duct of arbitrary but constant cross section.

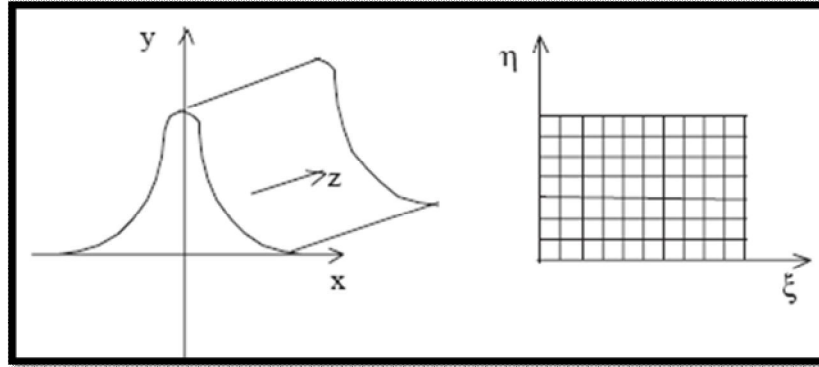


Fig.2 the transformation duct geometry from physical (x-y) plain to the computational plain (ξ-η).

The momentum and energy equations are solved numerically by neglecting the axial diffusion terms; therefore the resulting equations become parabolic and a two dimensional computational mesh can be constructed at each of the cross sections. For the above conditions, there is only one non-zero component of velocity (U) and constitutive equations of motion reduce to a single nonlinear partial differential equation of the form,

$$\frac{\partial}{\partial x} \left(\mu \frac{\partial u}{\partial x} \right) + \frac{\partial}{\partial y} \left(\mu \frac{\partial u}{\partial y} \right) = \frac{dp}{dz} \quad (1)$$

Where u: is the velocity component in the flow direction.

p: is the pressure.

μ: is the local viscosity coefficient at a point in the channel[Ashok 2001].

The power-law model is used in this study to describe the non-Newtonian behavior of the fluid, and consequently the expression for the local dimensionless viscosity at a point in the channel is given by:

$$\mu = m \left[\left(\frac{\partial u}{\partial x} \right)^2 + \left(\frac{\partial u}{\partial y} \right)^2 \right]^{(n-1)/2} \quad (2)$$

Where

$$\frac{\partial u}{\partial x} = \xi_x \frac{\partial u}{\partial \xi} + \eta_x \frac{\partial u}{\partial \eta} \quad (3)$$

$$\frac{\partial u}{\partial y} = \xi_y \frac{\partial u}{\partial \xi} + \eta_y \frac{\partial u}{\partial \eta} \quad (4)$$

where (n) is the index of the power-law, (m) is the consistency factor.

The dimensionless momentum equations (5) in the transformed coordinates can be written as,

$$J^{n+1} = (\alpha U_{\xi\xi} - 2\beta U_{\xi\eta} + \gamma U_{\eta\eta}) \cdot S \quad (5)$$

Where S is a variable viscosity and is given by the following equation,

$$S = \left[\left(\frac{\partial \xi}{\partial X} \frac{\partial U}{\partial \xi} + \frac{\partial \eta}{\partial X} \frac{\partial U}{\partial \eta} \right)^2 + \left(\frac{\partial \xi}{\partial Y} \frac{\partial U}{\partial \xi} + \frac{\partial \eta}{\partial Y} \frac{\partial U}{\partial \eta} \right)^2 \right]^{(n-1)/2} \quad (6)$$

Energy equation in Cartesian coordinate for a constant property neglecting axial conduction and viscous dissipation is,

$$\left[\frac{\partial}{\partial x} \left(\frac{\partial T}{\partial x} \right) + \frac{\partial}{\partial y} \left(\frac{\partial T}{\partial y} \right) \right] = u \frac{dT}{dz} \quad (7)$$

In dimensionless form,

$$\left[\frac{\partial}{\partial X} \left(\frac{\partial \theta}{\partial X} \right) + \frac{\partial}{\partial Y} \left(\frac{\partial \theta}{\partial Y} \right) \right] = \frac{U}{U_m} \frac{d\theta}{dZ} \quad (8)$$

Where

$$\left[\frac{\partial}{\partial X} \left(\frac{\partial \theta}{\partial X} \right) + \frac{\partial}{\partial Y} \left(\frac{\partial \theta}{\partial Y} \right) \right] = \frac{(\alpha T_{\xi\xi} - 2\beta T_{\xi\eta} + \gamma T_{\eta\eta})}{J^2} \quad (9)$$

The initial and boundary conditions of constant wall temperature, as shown,

$$\begin{aligned} \theta(0, \eta, \xi) &= 1 \\ \theta(z, 0, \xi) &= 0 \\ \theta(z, \eta, 0) &= 0 \end{aligned}$$

Velocity in entrance and boundary conditions is given as follows;

$$\begin{aligned} U &= 1.0 \quad Z=0 \\ U &= 0.0 \quad \xi=1 \text{ and } \xi=I \text{ for all } \eta \\ U &= 0.0 \quad \eta=1 \text{ and } \eta=J \text{ for all } \xi \end{aligned}$$

4. Numerical Solution Method:

The transformed governing equations (energy, momentum and continuity equations) are solved in rectangular computational domain using finite difference technique. The energy equation is linearized by setting the unknown to its value at the previous step, but the momentum and the continuity equations are solved only in axial direction. The indices (i,j,k) indicate positions in the (ζ,η,z) directions respectively. The axial step size (Δz) was taken as 5E-05. Starting with this value, subsequent this step size is gradually increased using the relation ΔZ_{n+1}=1.1* (ΔZ_n) until (Δz>1E-03); therefore the governing equations can be transferred with these indices as shown,

$$U_{\eta\eta} = \frac{U_{i,j+1} - 2U_{i,j} + U_{i,j-1}}{(\Delta\eta)^2} \tag{10}$$

$$U_{\xi\xi} = \frac{U_{i+1,j} - 2U_{i,j} + U_{i-1,j}}{(\Delta\xi)^2} \tag{11}$$

$$U_{\xi\eta} = \frac{U_{i+1,j+1} - U_{i+1,j-1} - U_{i-1,j+1} + U_{i-1,j-1}}{(4.\Delta\xi.\Delta\eta)} \tag{12}$$

$$\theta_{\xi\eta} = \frac{\theta_{i+1,j+1,k} - \theta_{i+1,j-1,k} - \theta_{i-1,j+1,k} + \theta_{i-1,j-1,k}}{(4.\Delta\xi.\Delta\eta)} \tag{13}$$

$$\theta_{\xi\xi} = \frac{\theta_{i+1,j,k} - 2\theta_{i,j,k} + \theta_{i-1,j,k}}{(\Delta\xi)^2} \tag{14}$$

$$\theta_{\eta\eta} = \frac{\theta_{i,j+1} - 2\theta_{i,j} + \theta_{i,j-1}}{(\Delta\eta)^2} \tag{15}$$

$$\theta_z = \frac{\theta_{i,j,k+1} - \theta_{i,j,k}}{\Delta Z} \tag{16}$$

To compute the velocity(U) and the temperature(θ)distribution, (n) which is the index of the flow behavior, is required. The initial value of (u) is (0.1) and increased by increment of 0.1 until maximum value of (n) reached to 1. It can be noted that the velocity values were determined only for the first step (K=1), but temperature values were computed at every step (K=1 to NK+1) in the axial direction for all index number. The over relaxation technique was used in computing velocity and temperature values.

The results from the preceding axial position (K) are substituted as initial values for the variables (K+1)th position. at any time, the fully developed velocity and developing temperature distribution. One obtained, the bulk mean temperature θ_b , the local Nusselt number Nu_T, and mean Nusselt number Nu_m , are computed, the following equations are employed at the axial position,

$$\theta_b = \frac{1}{Z.U_m} \int U.\theta.dZ \tag{17}$$

$$Nu(Z) = \frac{d\theta_b}{dZ} \frac{1}{-4.\theta_b} \tag{18}$$

5. Results and Discussion:

In order to verify the performance of the solution procedure, several test calculations were carried out. Firstly, the flow of Newtonian fluid was considered because numerical results are already available in previous studies. The numerical results were presented for comparison. In addition, numerical comparison of the elliptic grid generation technique and other methods also included. Excellent agreement was found between this work and the others. The mean Nusselt number for developing flow of a power-law fluid in square duct agreed with the constant property results of [Ashok and Sastri 2001]. Also there was excellent agreement with the results of [Ashok and Faghri 1988] for rhombic ducts with various angles [Uzun and Unsal 1997]. The limiting Nusselt number (Nu_T) for Newtonian fluids for a square ducts is presented in table1. The limiting Nusselt numbers (Nu_T), for ($0.4 \leq n \leq 1$) for hydrodynamically and thermally developing laminar flow of non-Newtonian fluid in triangular and square ducts are shown in the table 3. It is clear from tables 1 to 3 that the differences between the Nu_T values given in this study and those in previous investigations are less than 1-5%. The actual values of Nu_m and Nu_T selected at axial locations for different values of the power-law index ($n=1, n=0.4$) are shown in the tables 4 to 6. Three – dimensional fully developed velocity profiles for four-cusped and triangular ducts are presented in Figs.3a and 3b, respectively. As expected triangular dimensionless velocity values (U and U_{max}) are greater than those of four-cusped duct. Representative contours of axial fully developed velocity U are presented in Figs. 4a-c for triangular, Figures 5a and 5b depict the effect of the power law index (n) on the axial velocity profiles at selected axial location for triangular and four-cusped ducts respectively. Results for Nu_T and Nu_m as a function of the Graetz number are plotted in figs. 6a and 6b for triangular and trapezoidal ducts. The dashed lines in these figures indicate the local peripheral average Nusselt number Nu_T . The fully developed Nusselt number values are also plotted in these figures. Nu_T and Nu_m decrease with (z) and approach the fully developed values. The bulk temperature values are plotted in these figures. An extremely good agreement is obtained for fully developed values for triangular and square ducts.

6. Conclusions

From the present results, it can note that the Hydrodynamically fully developed and thermally developing laminar flow of non-Newtonian fluid in arbitrary cross-sectional ducts was analyzed. In order to eliminate the disadvantage of the non-uniform mesh and improve the numerical accuracy, the elliptic grid generation technique was used. The partial differential equations in Cartesian coordinates were transformed into the computational (ζ, η) domain. Inspection of the numerical solution shows that a non-Newtonian fluid with a flow behavior index of less than one gives a higher heat transfer coefficient than Newtonian fluid.

Table 1. Nu_T for Newtonian fluid for a square duct.

<i>Investigation</i>	<i>Nu_T</i>
Shah and London(1982)	2.976
Ashok andSastri (2001)	2.975
Asako and Faghri (1988)	2.976

Present study	2.972
----------------------	--------------

Table 2. Nusselts numbers for fully developed velocity and temperature profiles and square ducts for pseudo-plastic fluids.

<i>Power law Index, n</i>	<i>Nu_T, present study</i>		<i>Nu_T</i>	
	<i>Triangular</i>	<i>Square</i>	<i>Triangular Ashok(2001)</i>	<i>Square Shah (1982)</i>
1	2.355	2.971	2.340	2.975
0.9	2.383	2.821	-	2.997
0.8	2.399	3.029	-	3.030
0.7	2.444	3.033	-	3.070
0.6	2.481	3.231	-	3.120
0.4	2.555	3.288	-	3.184

Table 3. *Nu_T* and *Nu_m* for fully developed velocity and temperature profiles in a four-cusped duct and a square duct with four indented corners.

<i>Power law Index, n</i>	<i>4-cusped duct</i>		<i>Square duct with 4 indented corners</i>	
	<i>Nu_T</i>	<i>Nu_m</i>	<i>Nu_T</i>	<i>Nu_m</i>
1	1.0752	1.1365	2.0664	2.1233
0.9	1.0851	1.1471	2.0821	2.1415
0.8	1.0990	1.1602	2.1066	2.1664
0.7	1.1139	1.1755	2.1352	2.1955
0.6	1.1341	1.1957	2.1724	2.2436
0.4	1.1592	1.2222	2.2212	2.2819

Table 4. For sinusoidal ducts *Nu_T* and *Nu_m* versus axial direction, for a pseudo-plastic fluid.

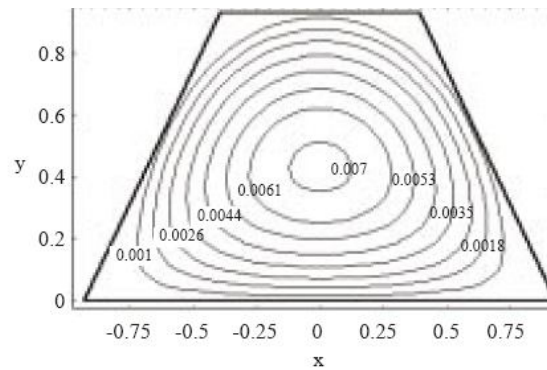
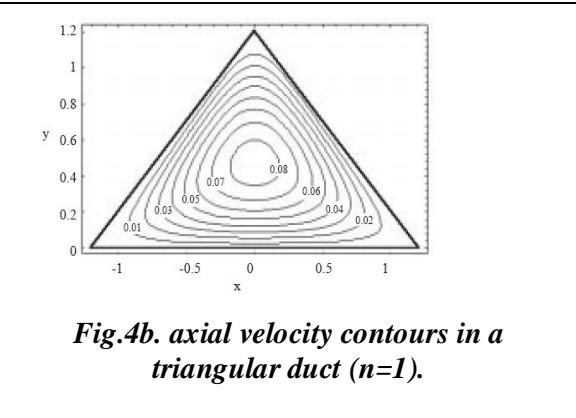
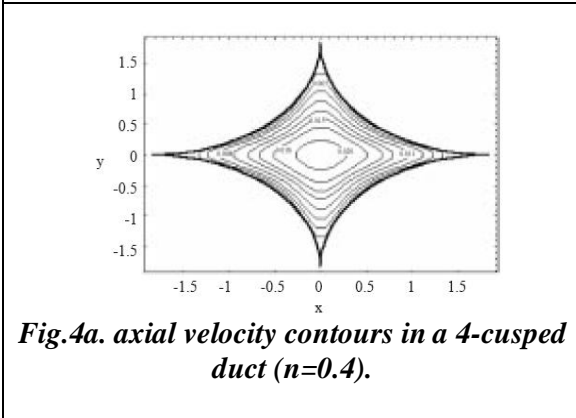
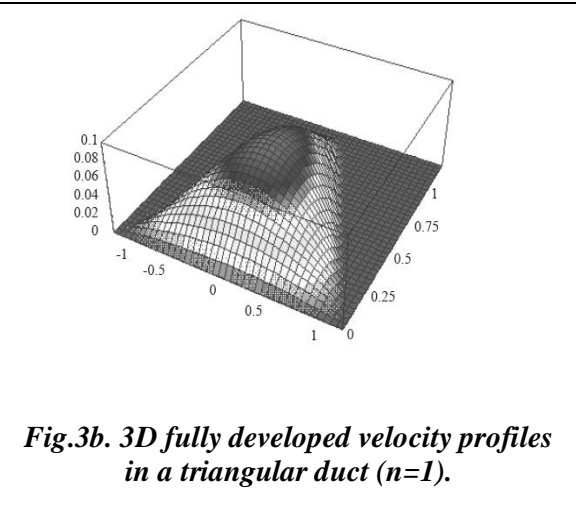
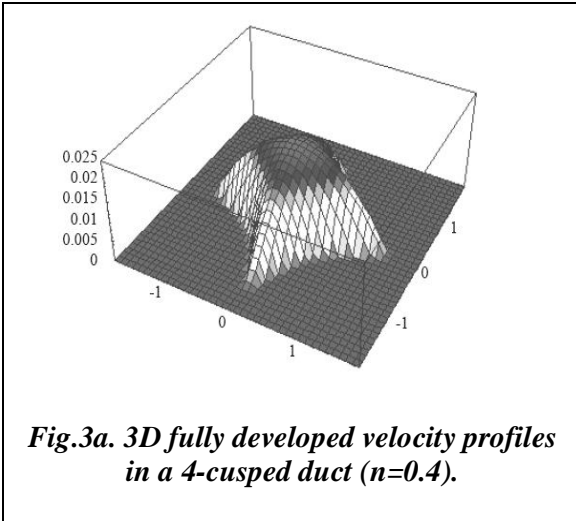
<i>Z</i>	<i>n=1.0</i>		<i>n=0.4</i>	
	<i>Nu_T</i>	<i>Nu_m</i>	<i>Nu_T</i>	<i>Nu_m</i>
$6.05 \cdot 10^{-5}$	19	19	21.631	21.631
$1.12 \cdot 10^{-3}$	13.72	14.87	15.412	17.532
$1.10 \cdot 10^{-2}$	7.81	10.214	8.302	11.212
$1.25 \cdot 10^{-1}$	3.378	4.928	3.612	5.244
0.1025	2.143	2.711	2.341	2.899
0.503	2.119	2.224	2.274	2.412
0.985	2.122	2.173	2.2788	2.302

Table 5. For triangular ducts Nu_T and Nu_m versus axial direction, for a pseudo-plastic fluid.

Z	$n=1.0$		$n=0.4$	
	Nu_T	Nu_m	Nu_T	Nu_m
6.05×10^{-5}	26.51	26.51	26.11	26.11
1.12×10^{-3}	18.61	21.55	18.91	21.71
1.10×10^{-2}	8.643	12.36	9.07	12.79
1.25×10^{-1}	3.741	5.521	3.972	5.802
0.1025	2.421	3.023	2.601	3.231
0.503	2.552	2.497	2.555	2.712
0.985	2.552	2.521	2.543	2.618

Table. 6. Nu_T and Nu_m , versus axial direction for pseudo-plastic fluid (0.4) in a four-cusped duct and a square duct with four indented corners.

Z	$n=1.0$		$n=0.4$	
	Nu_T	Nu_m	Nu_T	Nu_m
6.05×10^{-5}	12.766	12.766	22.341	22.341
1.12×10^{-3}	9.213	10.401	15.422	17.732
1.10×10^{-2}	5.263	6.887	8.103	11.056
1.25×10^{-1}	2.285	3.388	3.477	5.196
0.1025	1.212	1.716	2.266	2.813
0.503	1.158	1.256	2.221	2.345
1	1.162	1.231	2.221	2.288



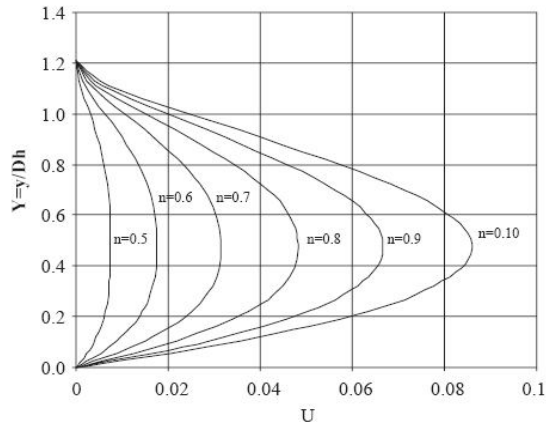


Figure 5a. Centerplane velocity profiles for non-Newtonian fluids in a triangular duct.

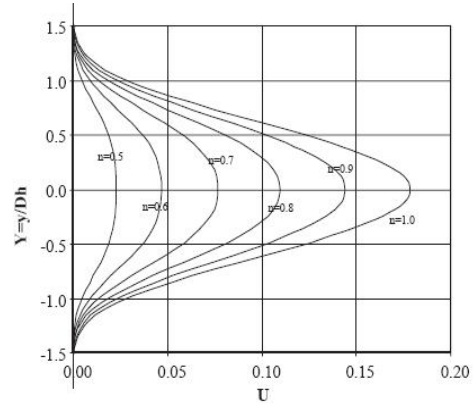


Figure 5b. Centerplane velocity profiles for non-Newtonian fluids in a four-cusped duct.

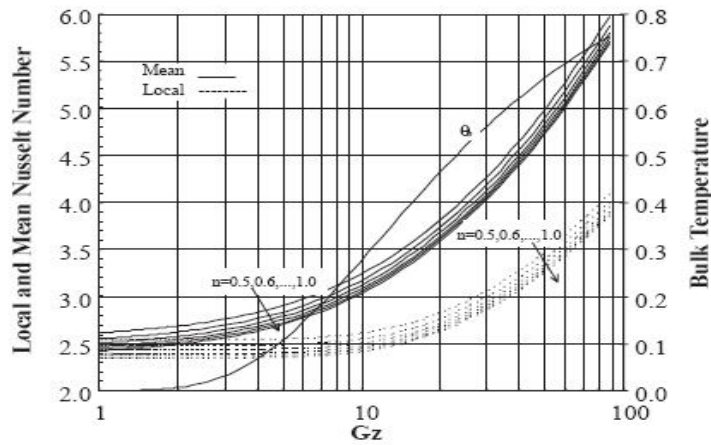


Figure 6a. Nusselt numbers and bulk temperature for power-law fluids in a triangular duct.

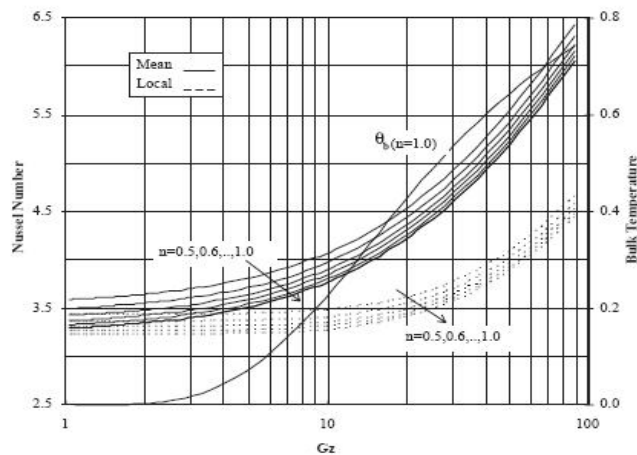


Figure 6b. Nusselt numbers and bulk temperature for power-law fluids in a trapezoidal duct.

References

Asako, Y. and Faghri, M. *"Three-Dimensional Laminar Heat Transfer and Fluid flow Characteristics in the entrance region of rhombic duct"*, J. Heat Transfer, 110, 855-861, 1988.

Ashok, R.C, and Sastri, V.M., *"Laminar forced Convection Heat Transfer of A Non-Newtonian Fluid in a Square Duct"*, Int. J.H.M.T., 20, 1315-1324, 2001.

Lawal, A., *"Mixed Convection Heat Transfer to Power Law Fluids in Arbitrary Cross-Sectional Ducts"*, J. Heat Transfer, 111, 399-406, 1999.

Nguyen, T.V., *"Laminar Heat transfer for thermally developing flow in ducts"*, Int.J.H.M.T., 35, 1733-1741, 1992.

Porter, J. E., *"Heat Transfer at Low Reynolds Number (Highly Viscous Liquids in Laminar flow)"*, Trans. Inst. Chem. Engrs, 49, 1-29, 2002.

Shah, R. K., and London, A. L., *"Laminar flow forced and convection heat transfer and flow friction in straight and curved ducts- a summary of analytical solutions"*, T.R., No.75, Stanford, 1982.

Shah, R.K., *"Laminar flow friction and forced convection in ducts of a arbitrary geometry"*, Int.J.H.M.T., 18, 849-862, 1981.

Syrjala S., *"Finite-Element Analysis of fully developed laminar flow of power-law Non-Newtonian Fluid in a rectangular duct"*, int. Comm. H.M.T., 22, 549-557, 1995.

Uzun, I. and Unsal, M., *"A Numerical Study of Laminar Heat Convection in Ducts of Irregular Cross-Sections"*, Int. Comm. H.M.T., 24, 835-848, 1997.